ISSN 1024-8560, Atmospheric and Oceanic Optics, 2017, Vol. 30, No. 1, pp. 33–38. © Pleiades Publishing, Ltd., 2017.
Original Russian Text © A.P. Kamardin, S.L. Odintsov, 2017, published in Optika Atmosfery i Okeana.

REMOTE SENSING OF ATMOSPHERE, HYDROSPHERE, AND UNDERLYING SURFACE

Height Profiles of the Structure Characteristic of Air Temperature in the Atmospheric Boundary Layer from Sodar Measurements

A. P. Kamardin and S. L. Odintsov*

V.E. Zuev Institute of Atmospheric Optics, Siberian Branch, Russian Academy of Sciences, Tomsk, 634055 Russia
**e-mail: odintsov@iao.ru*

Received April 4, 2016

Abstract—Results of the analysis of height profiles of the normalized structure characteristic of air temperature C_T^2 in the atmospheric boundary layer under conditions of daytime convection are discussed. The experimental data were obtained using the Volna-4M acoustic Doppler radar (sodar) in Akademgorodok district (Tomsk, Russia). The profiles were automatically normalized to the value of C_T^2 at the height $H = 100$ m. The analysis involved results obtained in daytime (11:00–16:00 LT) in a warm period (from July to August) of 2015. The shape of height profiles of C_T^2 obtained by the sodar are compared with similar profiles obtained by other authors. The presence of a break in the profiles of C_T^2 at heights of 60–80 m is noted.

Keywords: atmospheric boundary layer, sodar, structure characteristic of temperature
DOI: 10.1134/S1024856017010079

Studying height–time profiles of temperature turbulence characteristics in the atmospheric boundary layer (ABL) is an important problem in solving the general problem of optical radiation propagation in randomly inhomogeneous media. The method of remote acoustic sounding of the ABL is one of useful tools for solving this problem. Technical facilities implementing this method—meteorological acoustic radars (sodars)—are capable to provide measuring height–time profiles of the structure characteristic of temperature turbulence $C_T^2(H, t)$ in the ABL with a satisfactory spatiotemporal resolution. In solving various problems of atmospheric optics, a significant part is played by the structure characteristic of the refractive index of optical waves C_n^2, which is directly proportional to C_T^2. For this reason, results of the acoustic diagnostic of the ABL can be used for studying the conditions in which the use of optical devices is expected, as well as for interpreting results of optical observations [1–3]. For example, using sodars for testing possible sites for a three-meter astronomical telescope for estimating height profiles of C_T^2 and C_n^2, was considered in [4, 5]. A more detailed list of works related to remote acoustic sounding of the structure characteristic C_T^2 was presented in [6].

Height profiles of C_T^2 (and C_n^2) and models of these profiles in the boundary layer of the atmosphere have been a subject of research for many years. Different methods and technical facilities for measurements were applied, including lasers (see, e.g., [7]). Thus, at present one uses empirical models based on a power dependence on height: $C_n^2 \propto C_T^2 \propto H^m$. The exponent m for the ground layer can here be different from that in higher layers of the atmosphere. For example, in [3], for the ground layer ($H \le 50$ m), the value $m = -2/3$ is used; for the range of heights $50 < H \le 1000$ m, $m = -4/3$. The presence of a break in the profile of C_T^2 at low heights over the underlying surface seems to be caused by the change in the regime of temperature turbulence generation when passing from the ground layer of the atmosphere (its height is usually of 50–100 m) directly to the ABL "core." Note that the abovementioned model is applicable only for convective conditions in the ABL.

The main purpose of our work was to analyze the shape of height profiles of $C_T^2(H)$ obtained using a sodar under conditions of daytime convection in a warm season over an urbanized territory. The measurements were carried out using the Volna-4M sodar designed and manufactured in the Institute of Atmospheric Optics, Siberian Branch, Russian Academy of Sciences.

We briefly present the technique for determining $C_T^2(H, t)$ by results of acoustic sounding of the ABL. The sodar records the height–time distribution of the amplitude (an echogram) of a sound signal scattered by turbulent pulsations of air temperature in a mixture

with noise (instrumental and "external"): $A_S = A_C + A_N$, where A_C is the amplitude of the useful signal and A_N is the amplitude of the noise (in the reception band).

The structure characteristic of the temperature field $C_T^2(H, t)$ ($K^2\ m^{-2/3}$) in the boundary layer of the atmosphere is calculated based on the signal A_C by the formula [8, 9]:

$$C_T^2(H, t) = B_0(f)\tau f^{-1/3} T^{5/3}(H, t)H^2 \times \exp\left[2H\alpha_p(f, T, P, U)\right] A_C^2(H, f, t). \quad (1)$$

Here, $B_0(f)$ is the spread function which is determined upon the absolute calibration of the sodar; τ is the duration of the sounding pulse, s; f is the carrier frequency of the sound, Hz; T is the air temperature, K; H is the height, m; $\alpha_p(f, T, P, U)$ is the coefficient of sound power extinction, m^{-1}; P is the atmospheric pressure, Pa; and U is the relative humidity of air, %. The air temperature and humidity, as well as atmospheric pressure, depend on time and height.

The technique for determining the noise amplitude A_N was based on statistic estimates of its level in the reception band in height ranges where the useful signal was absent. At the first stage of purifying the signal from noise, it was assumed in an individual sounding act that $A_N = \text{const}$. After subtraction of the noise A_N from the initial signal A_S, an additional statistical analysis was performed; it allowed one to eliminate (in the main) the contribution of the nonstationary component of the noise.

The extinction coefficient $\alpha_p(f, T, P, U)$ was calculated using only near-ground data about meteorological parameters. Variation in these parameters with height was not taken into account. Possible errors appearing in this approach were discussed in [10, 11].

We have analyzed height profiles of C_T^2 obtained using the Volna-4M sodar in summer (July–August, 2015) in Tomsk (Akademgorodok district). The monitored height range was 45–700 m. We used echograms of a vertically oriented sounding channel at the carrier frequency of the signal $f = 2100$ Hz and duration of the sounding pulse $\tau = 150$ ms. For the analysis, measurements in the period 11:00–16:00 LT with a pronounced convective structure of the boundary layer of the atmosphere were chosen. In total, 24 episodes (days) of measurements have been processed. Note that the episodes for processing were chosen also using air temperature profiles obtained with an MTP-5 temperature profiler [12]. This device provided measurements of temperature profilers with height step of 50 m and time step of 5 min.

Figure 1a presents a typical example of an echogram purified from noises (A_C); Fig. 1b, an example of its transformation to $C_T^2(H, t)$ using formula (1).

For the further analysis of the shape of $C_T^2(H, t)$ profiles, it is more convenient to reduce them to the normalized form. For this purpose, $C_T^2(H, t)$ was automatically normalized to the value of this parameter at a height of 100 m. Since "instantaneous" profiles $C_T^2(H, t)$ are random to a large extent, they were preliminarily averaged over time intervals of 10 min. This averaging interval was chosen proceeding from the compromise between the problem of "tracking" the variability of the profile shape during an episode (day) of measurements and "statistical" nature of the parameter C_T^2. We also used a similar approach in the analysis of near-ground values of C_T^2 [13]. Figure 1c presents normalized and 10-min-averaged profiles $C_{Tn}^2(H, t_{10})$ corresponding to the distribution shown in Fig. 1b. From now on, the argument t_{10} pointing to the duration of the interval by which profiles of C_{Tn}^2 were determined is omitted.

As a rule, the profiles $C_T^2(H)$ and $C_n^2(H)$ were determined in different investigations as average values of these quantities for a rather long time interval. For example, the profiles $C_n^2(H)$ obtained in daytime in the near-ground layer as average values for 3–5 h were presented in [7]. It is such averaged profiles that served for the formulation of models of the form $C_n^2 \propto H^m$. We also averaged profiles $C_{Tn}^2(H)$ during the interval of 11:00–16:00 LT (we call them the daily average). Figure 1d presents the daily average profile $\overline{\log C_{Tn}^2(H)}$ obtained by profiles in Fig. 1c. The family of all 24 daily averaged profiles $\overline{\log C_{Tn}^2(H)}$ is presented in Fig. 2. Let us pay attention to the fact that an obvious systematic break of all profiles $\overline{\log C_{Tn}^2(H)}$ is observed in the height range 60–80 m.

In more details, the structure of profiles $C_{Tn}^2(H)$ can be studied by passing to the logarithm of this quantity and analyzing its relation to the logarithm of the height $\log H$. If we denote $y = \log C_{Tn}^2(H)$ and $x = \log H$, the derivative

$$y'_x = \partial \log C_{Tn}^2 / (\partial \log H) = m(H) \quad (2)$$

allows one to estimate the character of variation in $C_{Tn}^2(H)$ based on the formula

$$C_{Tn}^2(H) = CH^{m(H)}, \quad (3)$$

where C is a constant. An example of estimates $m(H)$ by formula (2) is presented in Fig. 3a. At heights above 250 m, the spread of values of m significantly increases. The initial profiles $C_{Tn}^2(H)$ based on which $m(H)$ were obtained are presented in Fig. 1c. Figure 3b

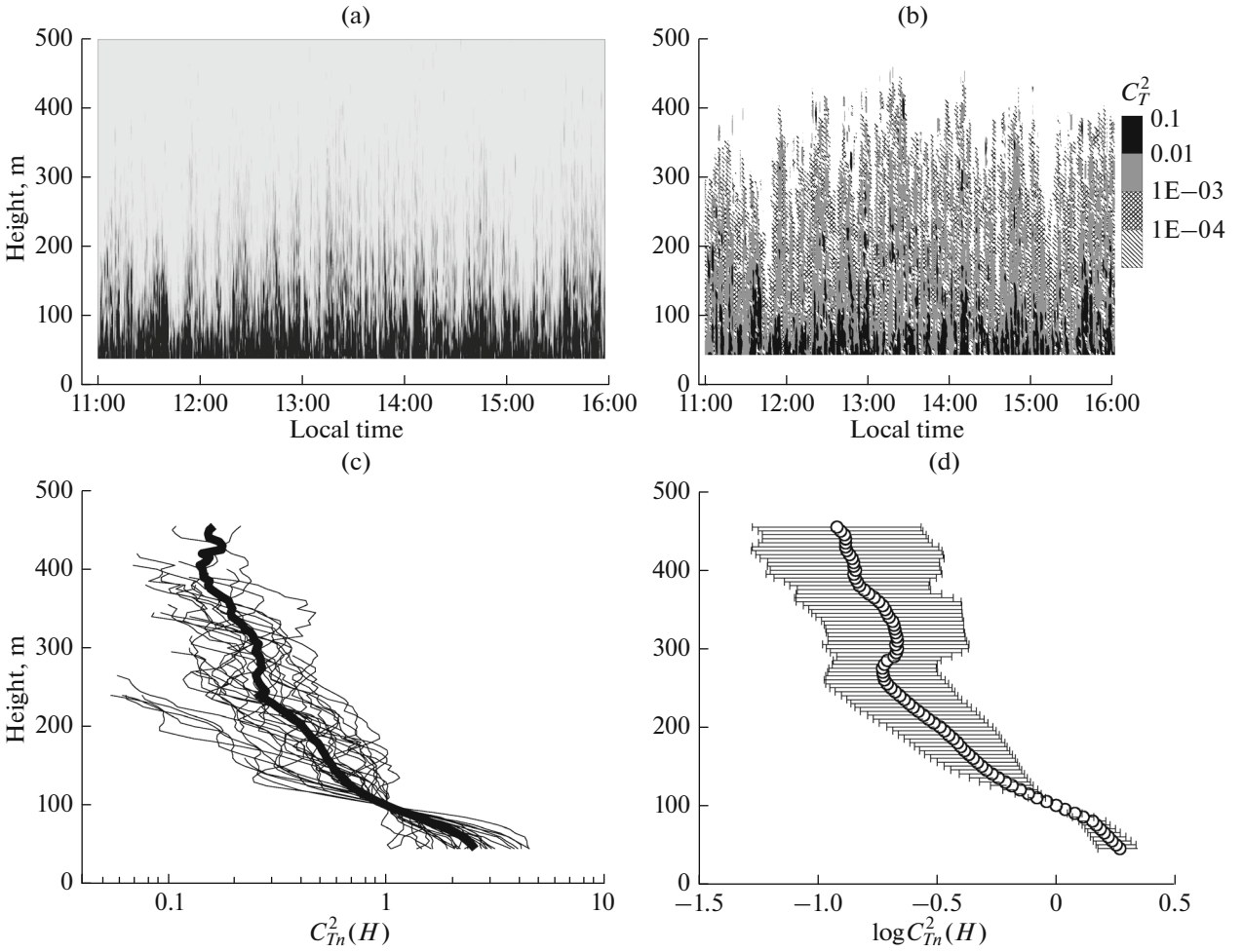

Fig. 1. (a) Echogram of the Volnas-4M sodar; (b) height-time distribution $C_T^2(H, t)$; (c) profiles $C_{Tn}^2(H)$ (thin lines) and (daily) average profile $\overline{C_{Tn}^2(H)}$ (heavy line); and (d) profile $\overline{\log C_{Tn}^2(H)}$ with the indication of the RMS deviation. July 20, 2015 (Tomsk, Akademgorodok district).

shows the daily averaged (median) profile $m_p(H)$. The average profiles $m_p(H)$ for each of 24 measurement episodes are presented in Fig. 3c. According to Fig. 3c, the shape of daily average profiles $m_p(H)$ is rather stable up to heights of about 300 m. Above this level, the spread of values of $m_p(H)$ significantly increases. The averaged shape of the profiles $m_p(H)$ over all 24 episodes of measurements is presented in Fig. 3d (denoted as $m_c(H)$).

The high degree of variability in daily average profiles $m_p(H)$ above the level of 300 m is apparently related to the high variability ("intermittency") of the structure of temperature inhomogeneities (see, e.g., Fig. 1b), to technical possibilities of the sodar used for measuring profiles of C_T^2 (insufficient potential according to the signal-to-noise criterion), as well as to the imperfection of the algorithm for processing the experimental data (separation of the useful signal A_C from the initial signal A_S). In the considered episodes, results obtained in the height range of up to 300 m can be treated as sufficiently reliable. In higher layers of the atmosphere, values of $m_p(H)$ should be considered only as estimates. Note that in the range 80–300 m both daily average profiles $m_p(H)$ and the total profile $m_c(H)$ over all measurement episodes are concentrated near the value $m = -4/3 \approx -1.33$.

As already mentioned, an obvious systematic break of all profiles $\overline{\log C_{Tn}^2(H)}$ is observed at a level of approximately 60–80 m (see Fig. 2). We assume that profiles $\overline{\log C_{Tn}^2(H)}$ can be approximated by linear functions above and below this level. It means that, in the height range 80–300 m, all daily average profiles $m(H)$ presented in Fig. 3c are concentrated near a certain constant value m_u; at heights below 80 m, near a constant value m_d. Results of linear approximations for

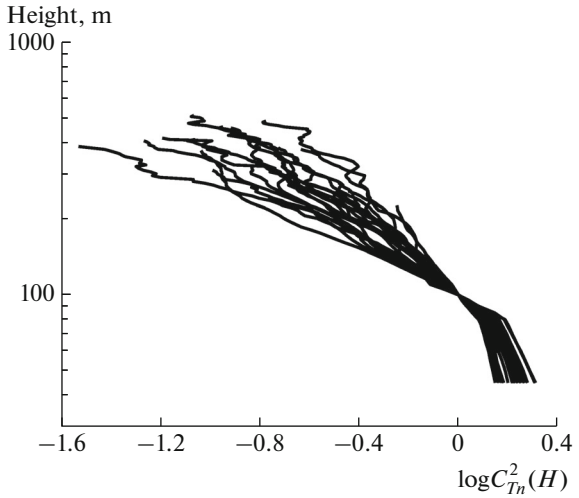

Fig. 2. Summary of normalized daily average profiles $\overline{\log C_{Tn}^2(H)}$.

the functions $\overline{\log C_{Tn}^2(H)}$ in height ranges above and below 80 m are presented in Fig. 4. Figure 4a shows linear approximations of profiles presented in Fig. 2; Fig. 4b, daily average values of the parameters m_u and m_d for 24 episodes of measurements. Dates of the performed measurements are shown on the abscissa in Fig. 4b. The dashed and solid lines in this figure are median values of m_u and m_d (−1.42 and −0.38, respectively).

The plots presented in Fig. 4a correspond to the model of height profiles of the form $C_T^2\,(C_n^2) \propto H^m$ with the presence of a break at a certain height in the near-ground layer. This result in general agrees with results of other authors. For example, in [7], experimental data on profiles $C_n^2(H)$ in the range of height below 80 m (measurements in summer in daytime over an even underlying surface) were presented. According

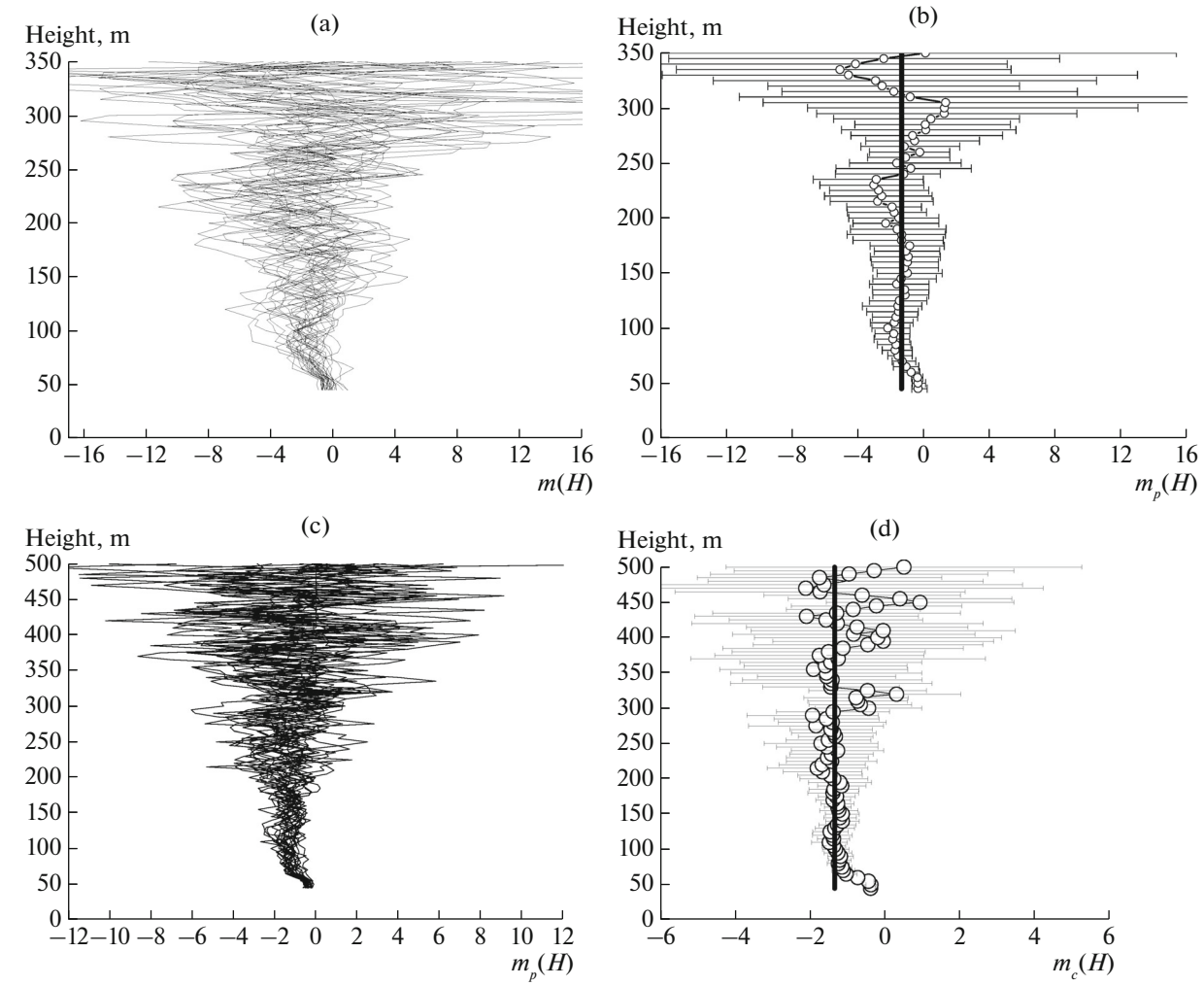

Fig. 3. (a) Family of profiles $m(H)$ according to results of measurements on July 20, 2015 (11:00–16:00 LT); (b) profile $m_p(H)$, average for July 20, 2015 (the segments show the RMS deviations); (c) profiles $m_p(H)$ for all days of observations (July–August, 2015, 11:00–16:00 LT); and (d) profile $m_c(H)$ averaged over all days of observations $m_c(H)$ (with the indication of the RMS deviation). The vertical line is the value $m = -4/3$.

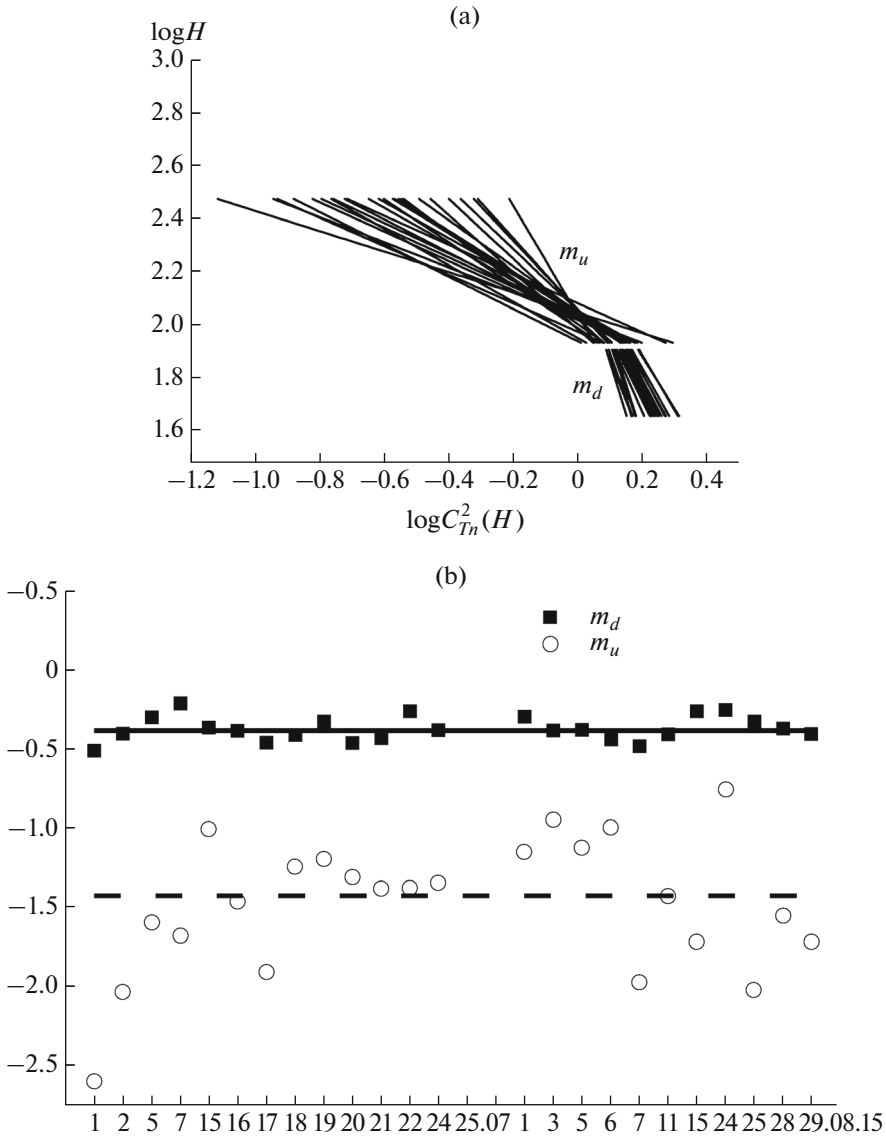

Fig. 4. (a) Linear approximations of $\log[\overline{C_{Tn}^2(\log H)}]$ in two height ranges (July–August, 2015, 11:00–16:00 LT) and (b) values of m_u and m_d.

to those results, variation in the profiles $C_n^2(H)$ in the layer below 30 m follows a law close to the power law with an exponent within the range $-0.33 \le m_d \le -0.66$. Above the level of 30 m, it also follows a power law but with an exponent (on the average) $m_u = -4/3 \approx -1.33$. Values of m_u and m_d presented in Fig. 4b are sufficiently close to similar values published in [7]. However, the level of the break in profiles of C_T^2 we obtained exceeds the level presented in [7] approximately by two times. This is probably related to the fact that our measurements were carried out over an urbanized territory where the dimensions of the near-ground layer and characteristics of turbulence in it can noticeably differ from conditions over an even underlying surface.

To summarize, one can draw the following main conclusions. First, the technique of remote acoustic sounding of the atmosphere can provide reliable estimates of the height profile of the structure characteristic of the temperature field (and of the structure characteristic of the refractive index of optical waves) with a satisfactory spatiotemporal resolution. Second, using the model profiles of C_T^2 (or C_n^2) of the form $C_T^2(H) \propto H^m$ with an a priori given value of m cannot correctly take into account the influence of temperature field pulsations when solving problems requiring

using current data on the quantities C_T^2 (or C_n^2) and their profiles because the current height distribution of the quantity under study can significantly differ from the model profile.

ACKNOWLEDGMENTS

This work was supported by the Ministry of Education and Science of the Russian Federation (agreement no. 14.604.21.0100, unique identifier RFMTFI60414X0100).

REFERENCES

1. V. P. Lukin, S. P. Ilyasov, V. V. Nosov, S. L. Odintsov, and Yu. A. Tillaev, "The study of astroclimate of the South Siberia and Central Asia regions," Opt. Atmos. Okeana **22** (10), 973–980 (2009).
2. V. V. Nosov, V. M. Grigoriev, P. G. Kovadlo, V. P. Lukin, E. V. Nosov, and A. V. Torgaev, "Recommendations for the site selection of sites for the ground-based astronomical telescopes," Opt. Atmos. Okeana **23** (12), 1099–1110 (2010).
3. N. N. Botygina, P. G. Kovadlo, E. A. Kopylov, V. P. Lukin, M. V. Tuev, and A. Yu. Shikhovtsev, "Estimation of the astronomical seeing at the large solar vacuum telescope site from optical and meteorological measurements," Atmos. Ocean. Opt. **27** (2), 142–146 (2014).
4. T. Travouillon, M. Schock, S. Els, R. Riddle, and W. Skidmore, "Using a sodar to measure optical turbulence and wind speed for the thirty meter telescope site testing. Part I: Reproducibility," Bound.-Lay. Meteorol. **141** (2), 273–288 (2011).
5. T. Travouillon, M. Schock, S. Els, R. Riddle, and W. Skidmore, "Using a sodar to measure optical turbulence and wind speed for the thirty meter telescope site testing. Part II: Comparison with independent instruments," Bound.-Lay. Meteorol. **141** (2), 289–300 (2011).
6. I. Petenko, G. Mastrantonio, A. Viola, S. Argentini, and I. Pietroni, "Some statistics of the temperature parameter in the convective boundary layer observed by sodar," Bound.-Lay. Meteorol. **150** (2), 215–233 (2014).
7. V. L. Mironov, *Laser Beam Propagation in a Turbulent Atmosphere* (Nauka, Novosibirsk, 1981) [in Russian].
8. V. A. Gladkikh and S. L. Odintsov, "Calibration of Volna-3 sodar," Atmos. Ocean. Opt. **14** (12), 1050–1053 (2001).
9. A. P. Kamardin and S. L. Odintsov, "Method for automatic absolute calibration of sodar measurement channels," Proc. SPIE—Int. Soc. Opt. Eng. **9680** (96805U) (2015). doi 10.1117/12.220532810.1117/12.2205328
10. I. V. Nevzorova, S. L. Odintsov, and V. A. Fedorov, "Some methodological aspects of sodar measurements of structural characteristic of temperature pulsation," in *Proc. 10th Int. Symp. on Acoust. Remote Sensing of the Atmosphere and Oceans. Auckland, New Zealand, 27 November – 1 December, 2000*, pp. 312–315.
11. V. A. Gladkikh, I. V. Nevzorova, and S. L. Odintsov, "VOLNA-3 sodar measurements of structure characteristic of atmospheric boundary layer," Proc. SPIE—Int. Soc. Opt. Eng. **4341**, 343–350 (2000).
12. E. N. Kadygrov, E. V. Ganshin, E. A. Miller, and T. A. Tochilkina, "Ground-based microwave temperature profilers: Potential and experimental data," Atmos. Ocean. Opt. **28** (6), 598–605 (2015).
13. V. A. Gladkikh, I. V. Nevzorova, S. L. Odintsov, and V. A. Fedorov, "Structure functions of air temperature over an inhomogeneous underlying surface. Part II. Statistics of structure functions' parameters," Atmos. Ocean. Opt. **27** (2), 154–163 (2014).

Translated by A. Nikol'skii